

Localization of Aquaporin-7 in Rat and Mouse Kidney Using RT-PCR, Immunoblotting, and Immunocytochemistry

L. N. Nejsun,* M.-L. Elkjær,* H. Hager,* J. Frøkiær,† T. H. Kwon,‡ and S. Nielsen*,¹

*Department of Cell Biology, Institute of Anatomy, University of Aarhus, DK-8000 Aarhus, Denmark; †Department of Experimental Physiology, Skejby Hospital, University of Aarhus, Aarhus, Denmark; and ‡Department of Physiology, School of Medicine, Dongguk University, Kyungju, 780-714 South Korea

Received August 29, 2000

To establish the segmental, cellular, and subcellular localization of AQP7 in rat and mouse kidney, we used RT-PCR, immunocytochemical, and immunoblotting approaches. RT-PCR of rat and mouse kidney zones revealed AQP7 mRNA in cortex and outer stripe of the outer medulla. RT-PCR on microdissected nephron segments revealed AQP7 mRNA in proximal convoluted and straight tubules. Immunoblotting using peptide-derived rabbit antibodies to either rat or mouse AQP7 revealed a 28-kDa band in kidney and testes from rat and mouse, respectively. Immunocytochemistry revealed strong AQP7 labeling of segment 3 proximal tubules and weaker labeling of proximal convoluted tubules in both rat and mouse kidneys. The labeling was almost exclusively confined to the brush border with no basolateral labeling. No labeling was observed of thin descending limbs or collecting duct. Immunolabeling controls were negative. The presence of AQP7 in the proximal tubule brush border indicates a role of AQP7 in proximal tubule water reabsorption.

© 2000 Academic Press

Aquaporin-7 (AQP7) was first cloned by Ishibashi and associates from rat testes (1) where it is localized in spermatids. AQP7 belongs, together with AQP3 (2, 3) and AQP9 (4), to the family of aquaporins transporting both water and glycerol. Consistent with this, AQP7 has the greatest amino acid homology with AQP3 (48% (2, 3) and AQP9 (47% (4)). Unlike most other aquaporins, AQP7 water permeability in oocytes

is not inhibited by high concentrations of mercury chloride (1).

So far several aquaporins have been identified in rat kidney. AQP1 was first cloned from human red blood cells (5) and is localized to the brush border and basolateral membrane in the proximal tubule (6). AQP2 was cloned from rat kidney (7) and is located in the apical part of collecting duct principal cells (8). AQP3 was cloned from rat (2, 3) and is located to the basolateral plasma membrane of the collecting duct principal cells (9, 10). AQP4 was cloned from rat (11, 12) and is located to the basolateral plasma membrane of the collecting duct principal cells (13). AQP6 was cloned from rat kidney (14) where it is located to intercalated cells of the kidney collecting duct in intracellular vesicles (15). So far, it remains unknown if AQP7 is present in kidney.

The purpose of this study was to investigate if AQP7 is present in kidney and then to define the eventual localization of AQP7 protein and mRNA in rat and mouse kidney. To accomplish this, we raised antibodies against peptides corresponding to the C-terminal part of rat and mouse aquaporin-7. We used these antibodies to locate the AQP7 protein in rat and mouse kidney using immunocytochemistry and immunoblotting. To localize mouse and rat AQP7 mRNA in the kidney, we designed sequence specific primers recognizing AQP7. RT-PCR was performed on rat and mouse kidney zones and on microdissected nephron segments from rat kidney.

MATERIALS AND METHODS

Experimental animals. Studies were performed on male Wistar rats weighing 180–260 g and NMRI mice weighing 35–40 g (Mølle-gard, Lille-Skensved, Denmark). The rats were maintained on standard rodent diet (Altromin, Lage, Germany) with free access to water.

Abbreviations used: aa, amino acid; AQP, aquaporin; bp, basepair; BSA, bovine serum albumin; ECL, enhanced chemiluminescence system; EDTA, ethylenediaminetetraacetic acid; SDS, sodium dodecyl sulfate; TRIS, tris(hydroxymethyl)-aminomethane.

¹To whom correspondence should be addressed. Fax: +45 86198664. E-mail: sn@ana.au.dk.

Antibodies. Polyclonal antibodies to rat AQP7 were raised in rabbits against a peptide corresponding to the following C-terminal amino acids: 259 to 269. Polyclonal antibodies to mouse AQP7 were raised in rabbits against peptides corresponding to the following C-terminal amino acids, antibodies 1 and 2: aa 283–303, antibodies 3 and 4: aa 254–284. The antibodies were affinity purified.

Membrane fractionation and immunoblotting. Tissues were homogenized (0.3 M sucrose, 25 mM imidazole, 1 mM EDTA, pH 7.2, containing 8.5 μ M leupeptin, 1 mM phenylmethylsulfonyl fluoride) using an ultra-Turrax T8 homogenizer (IKA Labortechnik, Staufen, Germany), and the homogenate was centrifuged in an Eppendorf centrifuge at 4000g for 15 min at 4°C to remove whole cells, nuclei, and mitochondria. The supernatant was then centrifuged at 200,000g for 1 h to produce a pellet containing membrane fractions enriched for both plasma membranes and intracellular vesicles. Gel samples (Laemmli sample buffer containing 2% SDS) were made of this pellet.

Electrophoresis and immunoblotting. Samples of membrane fractions from tissues were run on 12% polyacrylamide minigels (Bio-Rad Mini Protean II). The gel was subjected to immunoblotting. After transfer by electroelution to nitrocellulose membranes, blots were blocked with 5% milk in PBS-T (80 mM Na₂HPO₄, 20 mM NaH₂PO₄, 100 mM NaCl, 0.1% Tween 20, pH 7.5) for 1 h, and incubated with primary antibodies (see above). The labeling was visualized with horseradish peroxidase (HRP)-conjugated secondary antibody (P448, DAKO, Glostrup, Denmark, diluted 1:3000) using enhanced chemiluminescence system (Amersham Pharmacia Biotech, Hørsholm, Denmark). Immunolabeling controls were performed using peptide-absorbed antibody, as previously described (16, 17).

Immunohistochemistry. Male Wistar rats (weighing 250–300 g) and male NMRI mouse (weighing 35–40 g) were anaesthetized with halothane and were fixed by retrograde perfusion through the abdominal aorta with 2 or 4% paraformaldehyde with or without 0.1% glutaraldehyde in 0.1 M sodium cacodylate buffer. The kidneys, testes, and epididymis were removed and postfixed for 1 h. For preparation of semithin sections (0.8–1 μ m, Reichert Ultracut S Cryoultramicrotome), tissue blocks were infiltrated for 30 min with 2.3 M sucrose containing 2% paraformaldehyde, mounted on holders, and rapidly frozen in liquid nitrogen. For preparation of cryostat sections (10 μ m), tissues were cryoprotected in 25% sucrose. For paraffin sections kidney blocks containing all kidney zones were dehydrated and embedded in paraffin. The paraffin embedded tissue was cut at 2 μ m on a rotary microtome (Micon, Germany). The staining was carried out using indirect immunoperoxidase method. The sections were dewaxed and rehydrated. For immunoperoxidase labeling, endogenous peroxidase were blocked by 0.5% H₂O₂ in absolute methanol for 10 min at room temperature. To reveal antigens, sections were put in 1 mmol/liter Tris solution (pH 9.0) supplemented with 0.5 mM EGTA and were heated using a microwave oven for 10 min. Nonspecific binding of immunoglobulin was prevented by

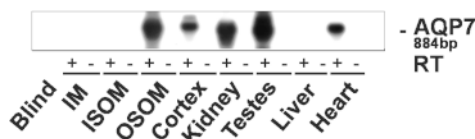


FIG. 1. AQP7 RT-PCR on total RNA isolated from mouse kidney zones. Southern blot shows AQP7 signal in outer stripe of the outer medulla (OSOM) and cortex, whereas no signal was observed in inner medulla (IM) or inner stripe of the outer medulla (ISOM) (presence of cDNA in all samples was confirmed with β -actin, not shown).

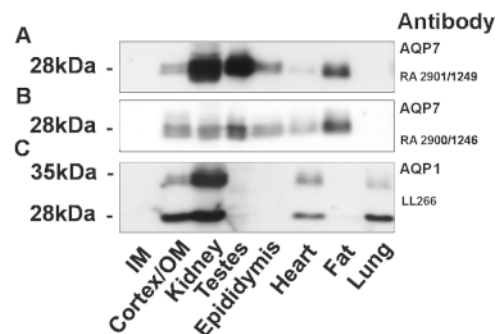


FIG. 2. Two different anti-mouse-AQP7 antibodies recognize a 28-kDa band in membrane fractions from mouse kidney (inner medulla, cortex/outer medulla (OM) or total kidney), testes, epididymis, heart, and perirenal fat. (A) Both anti-AQP7 antibodies 2901/1249 and 2900/1246 specifically recognize a ~28 kDa band in mouse cortex and OM, whole kidney, testes, epididymis, heart, and perirenal fat. (B) Anti-AQP1 specifically recognizes an ~28-kDa band, corresponding to the nonglycosylated form of AQP1, and a 35- to 50-kDa band, corresponding to the glycosylated form of AQP1, in mouse cortex and OM, whole kidney, heart, and lung.

incubating the sections in 50 mM NH₄Cl in 30 min followed by blocking in PBS supplemented with 1% BSA, 0.05% saponin, and 0.2% gelatin. Sections were incubated overnight at 4°C with primary antibodies diluted in PBS supplemented with 0.1% BSA and 0.3% Triton X-100. After rinsing with PBS supplemented with 0.1% BSA, 0.05% saponin and 0.2% gelatin for 3 \times 10 min the sections were washed (see above) followed by incubation in horseradish peroxidase-conjugated goat anti-rabbit immunoglobulin (DAKO P448) diluted in PBS supplemented with 0.1% BSA and 0.3% Triton X-100. The microscopy was carried out using a Leica DMRE light microscope.

Microdissection of rat nephron segments. Kidneys from normal male Wistar rats (180–200 g) were perfused with saline via the abdominal aorta followed by perfusion with collagenase A in DMEM medium (Life Technologies, Tåstrup, Denmark) with 0.1% BSA, 1 ml/liter penicillin-streptomycin solution (Sigma Chemical) and 660 U/liter insulin. Kidney slices were further incubated for 25 min at 37°C with gently shaking. The slices were moved to DMEM containing 10% fetal calf serum and tubules (20 mm of each segment) were dissected on ice using a Leica MZ 12.5 microscope.

RNA extraction. mRNA was extracted from tissues or dissected nephron segments using poly-T-coated magnetic beads (Dynabeads mRNA DIRECT Micro kit, Dynal, Oslo, Norway) or total RNA was extracted using RNA Plus (Quantum Biotechnologies SA, Monteuil Cedex, France).

RT-PCR and Southern blotting. Reverse transcriptase was performed on mRNA (directly on the magnetic beads) or total RNA using Superscript II (Life Technologies, Tåstrup, Denmark), both RT positive (RT+, addition of reverse transcriptase) and RT negative (RT-, no addition of reverse transcriptase) were performed. PCR (30 cycles) test for β -actin was performed to confirm the presence of cDNA. PCR (30 cycles) was performed using sequence specific primers for AQP7 (AQP7 sense 5'-CCACAATGGCCGGTCTGTG-3', AQP7 antisense 5'-CCAATCTCTAAGAACCCTGT-3'). The addition of cDNA was normalized with respect to the β -actin bands. A PCR control (PCR without the addition of cDNA), was performed with every PCR. PCR products were separated on a 2% agarose gel in 1 \times TBE and the products were visualized with ethidium bromide. The gel was incubated for 15 min in 1.5 M NaCl, 0.5 M NaOH to denature the PCR

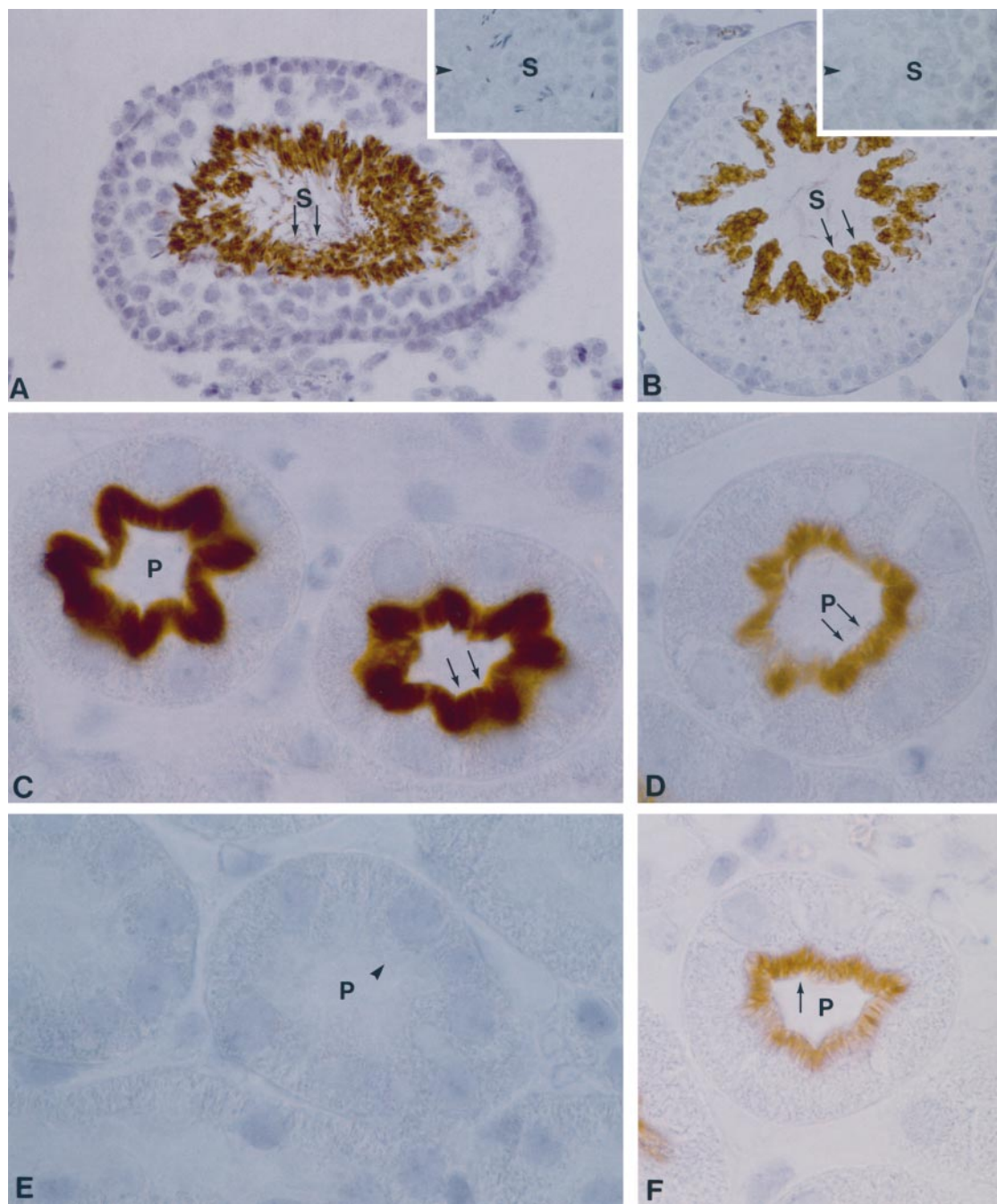


FIG. 3. Anti-mouse-AQP7 antibody labels mouse kidney and testes using paraffin sections (2- to 3- μ m sections). (A and B) Two different anti-AQP7 antibodies (A, 2900/1246; B, 2900/1247) label spermatogenic cells (S) in mouse testes (arrows). Insets show immunolabeling controls using anti-AQP7 antibodies preabsorbed with the respective immunizing peptide. No labeling is seen. (C, D, and F) Three different anti-AQP7 antibodies (C, 2900/1246; D, 2900/1247; F, 2901/1248) label the brush border in segment 3 in the proximal tubule (P) in mouse kidney (arrow). (E) Immunolabeling control using anti-AQP7 (2900/1246) preabsorbed with immunizing peptide shows absence of labeling (arrowhead) in proximal tubule (P). Magnification: A and B, $\times 250$; C-F, $\times 1100$.

products followed by a 15-min neutralization in 1.5 M NaCl, 0.5 M Tris, 0.77% HCl. The PCR products were transferred to positively charged membranes (Roche, Hvidovre, Denmark) by capillary transfer overnight in $10\times$ SSC. The PCR products were crosslinked to the membrane using an UV crosslinker (Amersham Pharmacia Biotech, Hørsholm, Denmark). For detection of the PCR products we used

Gene Images CDP-Star detection module (#RPN 3510, Amersham Pharmacia Biotech, Hørsholm, Denmark). Blots were placed in a glass hybridization tube containing $5\times$ SSC, 0.1% (w/v) SDS, 5% dextran sulphate and 20-fold dilution of liquid block reagent. Prehybridization was performed at 60°C for 30 min in a hybridization oven. The fluorescein-labeled AQP7 cDNA probe labeled using Gene

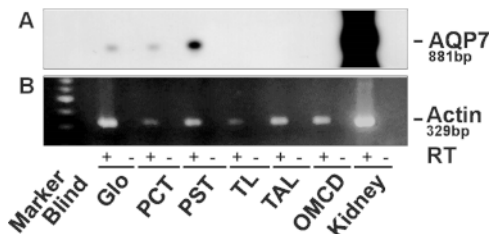


FIG. 4. AQP7 RT-PCR on mRNA isolated from microdissected nephron and collecting duct segments and on total RNA isolated from rat kidney. (A) Southern blot showing AQP7 RT-PCR signal in proximal convoluted tubule (PCT), proximal straight tubule (PST), and glomerulus (Glo) and total kidney (kidney). (B) Presence of cDNA in all samples was confirmed with β -actin.

Images random prime labeling module (#RPN 3540, Amersham Pharmacia Biotech, Hørsholm, Denmark) was then added and membranes were incubated overnight at 60°C. The blots were washed once at 60°C in 1× SSC, 0.1% SDS for 15 min, and once at 60°C in 0.5× SSC, 0.1% SDS for 15 min. Blots were blocked for 1 h with liquid block reagent diluted 1:10 in buffer A (100 mM Tris-HCl, 300 mM NaCl, pH 9.5). After incubation for 1 h with anti-fluorescein-AP conjugate diluted 1:5000 in buffer A with 0.5% (w/v) BSA blots were washed three times for 15 min in buffer A containing 0.3% Tween 20. The bands were visualized using the chemiluminescent substrate, CDP-star.

RESULTS

RT-PCR and Southern blotting of mouse kidney. For a sensitive evaluation of the localization of AQP7 mRNA in kidney, AQP7 RT-PCR followed by Southern blotting with an AQP7-specific probe was performed on dissected mouse kidney zones (Fig. 1). AQP7 mRNA was located in the outer stripe of the outer medulla and in cortex, but was absent in the inner stripe of the outer medulla and in the inner medulla. The presence of cDNA was confirmed with an β -actin PCR test (not shown).

Immunoblotting and immunocytochemistry of mouse kidney. To examine the protein localization of AQP7, immunoblotting was performed using two different mouse anti-AQP7 antibodies. The mouse anti-AQP7 antibodies recognize a 28-kDa band in control tissue known to express AQP7 (1) and include mouse testes, epididymis, heart, and perirenal fat (Figs. 3A and 3B). Immunoblotting of mouse kidney zones revealed a 28-kDa band in mouse cortex/outer medulla (OM) but no AQP7 labeling was detected in the inner medulla (Figs. 2A and 2B) consistent with RT-PCR results. Preabsorption control with the immunizing peptide completely ablated the 28-kDa band (not shown). Immunocytochemistry using the same antibodies against mouse AQP7 (Fig. 4), revealed strong labeling of the spermatids in mouse testes (Figs. 3A and 3B) and epididymis (not shown) consistent with the finding of Ishibashi and colleagues (1). All four antibodies gave

the same labeling. These antibodies also labeled the proximal tubule brush border in mouse kidney (Figs. 4C, 4D, and 4E). The labeling was strongest in segment 3 of the proximal tubule with weaker labeling of the brush border in segment 2 and 1 (not shown). All four antibodies raised against two different mouse AQP7 peptides gave the same labeling of proximal tubules. Preabsorption control with the immunizing peptide completely ablated the labeling (Figs. 4A and 4B, insets).

RT-PCR and immunocytochemical localization of rat AQP7 in the kidney. To substantiate the AQP7 findings in mouse kidney we performed RT-PCR on mouse kidney zones and on dissected nephron and collecting duct segments and immunocytochemistry of rat kidney. RT-PCR on dissected rat kidney zones followed by Southern blotting with an AQP7 specific probe confirmed the findings in mouse. AQP7 was observed in the cortex and the outer stripe of the outer medulla in rat kidney (not shown). To further locate AQP7 mRNA, AQP7 RT-PCR was performed on microdissected nephron segments and collecting duct from rat kidney (Fig. 4). AQP7 mRNA was located to the proximal convoluted tubule and the proximal straight tubule. Also AQP7 mRNA was located by this method to the glomeruli, but immunolabeling using anti-AQP7 showed no labeling of the glomeruli (not shown). We believe the AQP7 mRNA found in the glomeruli is due to the presence of proximal convoluted tubule in the dissected glomeruli. No AQP7 mRNA was located in the thin limb or in the outer medulla collecting duct. The presence of cDNA in all samples was confirmed with a β -actin PCR test (Fig. 4B).

Immunocytochemistry using an antibody raised against rat AQP7 showed the same labeling pattern as observed in mouse. The antibody labeled the spermatids of rat epididymis (Figs. 5A and 5B) and rat testes (Figs. 5C and 5D) consistent with findings from Ishibashi and colleagues (1). Rat anti-AQP7 also labeled the brush border in the proximal tubule in rat kidney (Figs. 5E and 5F). The labeling was strongest in segment 3 of the proximal tubule with weaker labeling of the brush border in segment 2 and 1 (not shown). Preabsorption control with the immunizing peptide completely ablated the labeling (Fig. 5E, inset).

DISCUSSION

In the present study, we demonstrated that AQP7 is present in mouse and rat kidney where it is exclusively present at the apical brush border of the proximal tubules. Immunoblotting using peptide-derived polyclonal antibodies raised against mouse and rat AQP7 revealed a distinct ~28-kDa band in the membrane fractions of mouse and rat kidney, in addition to testis.

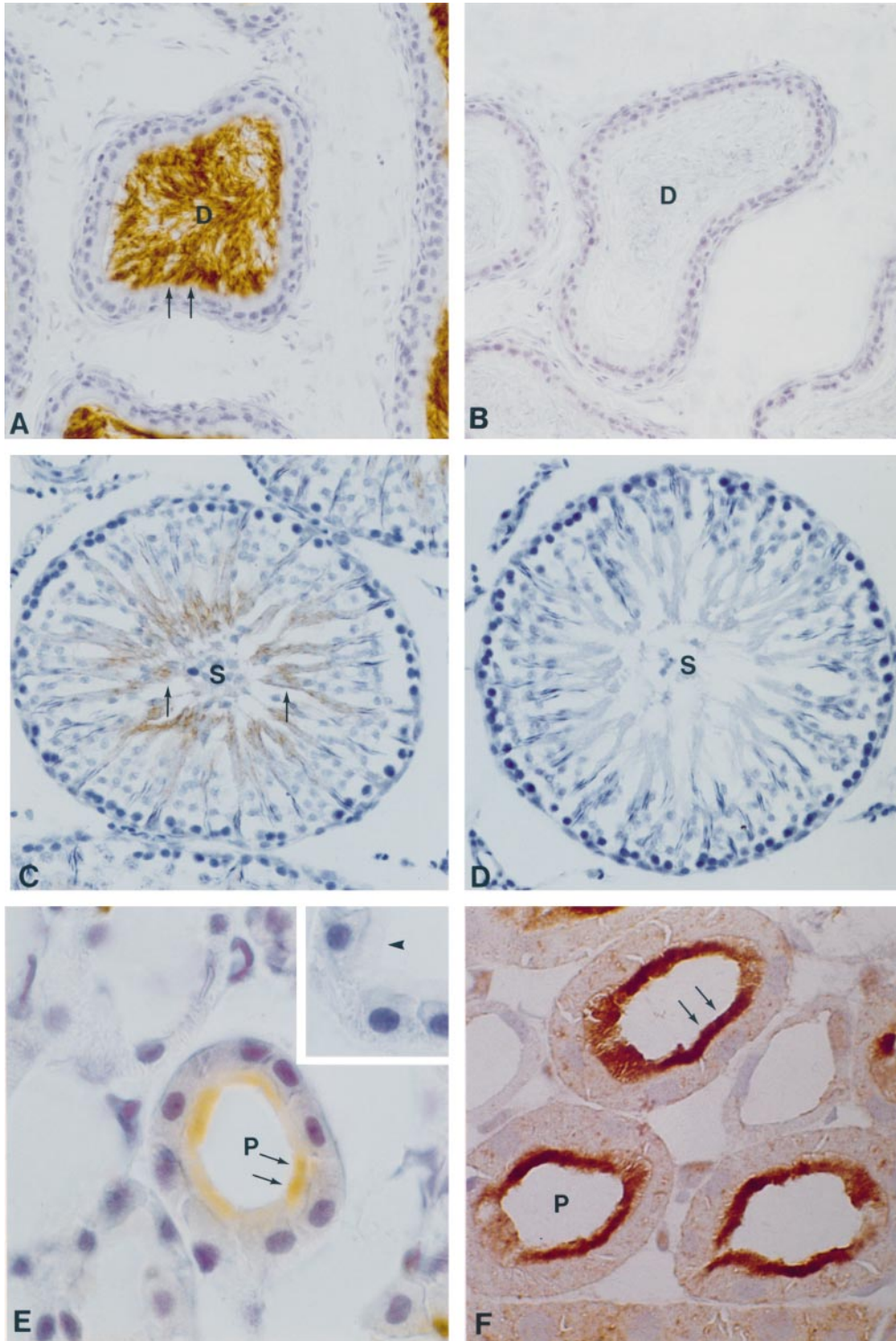


FIG. 5. Anti-rat-AQP7 antibody labels rat kidney, testes, and epididymis on semithin cryosections (10- μ m sections). (A) Anti-AQP7 labels spermatogenic cells in rat epididymis (arrows). (B) Immunolabeling control using anti-AQP7 antibody preabsorbed with immunizing peptide shows absence of labeling. (C) Anti-AQP7 antibody labels spermatogenic cells in rat testes (arrows). (D) Immunolabeling control of rat testes using anti-AQP7 preabsorbed with immunizing peptide shows absence of labeling. (E) Anti-AQP7 labels the brush border in segment 3 in the proximal tubule in rat kidney (arrow). (Inset, preabsorption control shows no labeling). (F) Anti-AQP7 antibody labels the brush border in segment 2 in the proximal tubule in rat kidney (arrow). Magnification: A–D, $\times 250$; E and F, $\times 650$.

Immunoperoxidase microscopy revealed the exclusive labeling of AQP7 at the apical plasma membranes of the proximal tubules including brush border, particularly in segment 3 proximal tubules. RT-PCT Southern blot analyses of microdissected mouse and rat kidney nephron confirmed the presence of AQP7 mRNA in the proximal convoluted tubules as well as proximal straight tubules. The presence of AQP7 in the proximal tubules of mouse and rat kidney therefore indicates a potential role of AQP7 in the proximal tubule water reabsorption. Proximal tubule epithelia carry out active sodium reabsorption mainly through apically expressed Na/H exchanger and basolaterally expressed Na,K-ATPase. Since proximal tubule has an extraordinary high water permeability (18–20), which is chiefly mediated by the transcellular water movement through AQP1 (6), the water flow can occur at rates proportional to active sodium absorption. Recently several studies have emphasized the critical role of AQP1 in the constitutive water reabsorption in the proximal tubules and thin descending limbs of Henle (21, 22). Importantly, Schnermann *et al.* (21) have demonstrated that the epithelial osmotic water permeability of segment 2 proximal tubules from AQP1 knockout mice is about 20% of the value in wild-type mice. This suggests that AQP1 accounts for about 80% of the osmotic water permeability in the proximal tubule.

Hence, it has been proposed that the residual water permeability may largely occur by water movement through the lipid portion of the membrane (21). Moreover, it was previously reported that the osmotic water permeability is reduced by 89% at 10°C in purified apical plasma membrane vesicles from proximal tubules in AQP1 knockout mice versus wild-type mice and that the remaining low water permeability in vesicles from the knockout mice was not inhibited by mercurial (23). Thus this potentially may reflect lipid permeation or potentially via a mercurial-insensitive pathway (e.g., via a mercurial insensitive aquaporin). AQP7, which was identified from rat testis, has the highest amino acid sequence identity with AQP3 (47%). The osmotic water permeability coefficient (Pf) of AQP7-cRNA-injected oocytes is 10 times higher than that of water-injected oocytes, and this is comparable to the levels of other aquaporins (1). However, interestingly this high water permeability of AQP7 in oocytes is not inhibited by mercury chloride. Moreover AQP7 also facilitate glycerol and urea transport, as do AQP3 (1). Thus based on the mercurial insensitivity of AQP7 and its location in the proximal tubule brush border it is likely that AQP7 may be partly responsible for the residual mercurial-insensitive osmotic water permeability in brush border membranes prepared from kidneys of AQP1-knock-out mice.

Recently, it has been demonstrated that in mice (in contrast to the rat) AQP4 is present in the basolateral

plasma membrane of S3 proximal straight tubules (in addition to being present in the collecting duct principal cells (24). Thus, together with this, our data showing the localization of AQP7 at the apical brush border of the proximal tubule may suggest that part of the residual water permeability of the proximal tubules in AQP1 knockout mice (i.e., the mercurial insensitive pathway (23) could be mediated by apically expressed AQP7 and basolaterally expressed AQP4, particularly in the S3 proximal straight tubules. Hence future studies are needed to investigate the role of AQP7 in the proximal tubule water reabsorption and to test whether AQP7 is regulated in response to altered water metabolism. This may potentially be achieved by development of transgene mice lacking AQP7.

In conclusion, the present study demonstrated that AQP7 is present in the straight proximal tubule where it is speculated to play a role together with AQP1 for the proximal tubule water reabsorption.

ACKNOWLEDGMENTS

We thank Inger Merete Paulsen, Zhila Nikrozi, Gitte Christensen, Helle Høyer, and Mette Frank Vistisen for excellent technical assistance. This work was supported by the Danish Research Academy, the Karen Elise Jensen Foundation, the Novo Nordisk Foundation, the Danish Medical Research Council, the University of Aarhus Research Foundation, the University of Aarhus, the Helen and Ejnar Bjørnøw's Foundation, the A. P. Møller and Spouse Chastine McKinney Møllers Foundation, the Mrs. Ruth T. E. König-Petersens Research Foundation for Kidney Diseases, and the Research Foundation of the Danish Kidney Assoc.

REFERENCES

1. Ishibashi, K., Kuwahara, M., Gu, Y., Kageyama, Y., Tohsaka, A., Suzuki, F., Marumo, F., and Sasaki, S. (1997) *J. Biol. Chem.* **272**, 20782–20786.
2. Echevarria, M., Windhager, E. E., Tate, S. S., and Frindt, G. (1994) *Proc. Natl. Acad. Sci. USA* **91**, 10997–11001.
3. Ishibashi, K., Sasaki, S., Fushimi, K., Uchida, S., Kuwahara, M., Saito, H., Furukawa, T., Nakajima, K., Yamaguchi, Y., Gojobori, T., and Marumo, F. (1994) *Proc. Natl. Acad. Sci. USA* **91**, 6269–6273.
4. Ko, S. B., Uchida, S., Naruse, S., Kuwahara, M., Ishibashi, K., Marumo, F., Hayakawa, T., and Sasaki, S. (1999) *Biochem. Mol. Biol. Int.* **47**, 309–318.
5. Preston, G. M., and Agre, P. (1991) *Proc. Natl. Acad. Sci. USA* **88**, 11110–11114.
6. Nielsen, S., Smith, B., Christensen, E. I., Knepper, M. A., and Agre, P. (1993) *J. Cell Biol.* **120**, 371–383.
7. Fushimi, K., Uchida, S., Hara, Y., Hirata, Y., Marumo, F., and Sasaki, S. (1993) *Nature* **361**, 549–552.
8. Nielsen, S., DiGiovanni, S. R., Christensen, E. I., Knepper, M. A., and Harris, H. W. (1993) *Proc. Natl. Acad. Sci. USA* **90**, 11663–11667.
9. Ecelbarger, C. A., Terris, J., Frindt, G., Echevarria, M., Marples, D., Nielsen, S., and Knepper, M. A. (1995) *Am. J. Physiol.* **269**, F663–F672.

10. Frigeri, A., Gropper, M. A., Turck, C. W., and Verkman, A. S. (1995) *Proc. Natl. Acad. Sci. USA* **92**, 4328–4331.
11. Jung, J. S., Bhat, R. V., Preston, G. M., Guggino, W. B., Baraban, J. M., and Agre, P. (1994) *Proc. Natl. Acad. Sci. USA* **91**, 13052–13056.
12. Hasegawa, H., Ma, T., Skach, W., Matthay, M. A., and Verkman, A. S. (1994) *J. Biol. Chem.* **269**, 5497–5500.
13. Terris, J., Ecelbarger, C. A., Marples, D., Knepper, M. A., and Nielsen, S. (1995) *Am. J. Physiol.* **269**, F775–F785.
14. Ma, T., Frigeri, A., Skach, W., and Verkman, A. S. (1993) *Biochem. Biophys. Res. Commun.* **197**, 654–659.
15. Yasui, M., Kwon, T. H., Knepper, M. A., Nielsen, S., and Agre, P. (1999) *Proc. Natl. Acad. Sci. USA* **96**, 5808–5813.
16. Nielsen, S., Nagelhus, E. A., Amiry-moghaddam, M., Bourque, C., Agre, P., and Ottersen, O. P. (1997) *J. Neurosci.* **17**, 171–180.
17. Wen, H., Nagelhus, E. A., Amiry-moghaddam, M., Agre, P., Ottersen, O. P., and Nielsen, S. (1999) *Eur. J. Neurosci.* **11**, 935–945.
18. Schafer, J. A., Troutman, S. L., Watkins, M. L., and Andreoli, T. E. (1978) *Am. J. Physiol.* **234**, F332–F339.
19. Schafer, J. A., Patlak, C. S., Troutman, S. L., and Andreoli, T. E. (1978) *Am. J. Physiol.* **234**, F340–F348.
20. Andreoli, T. E., Schafer, J. A., and Troutman, S. L. (1978) *Kidney Int.* **14**, 263–269.
21. Schnermann, J., Chou, C. L., Ma, T., Traynor, T., Knepper, M. A., and Verkman, A. S. (1998) *Proc. Natl. Acad. Sci. USA* **95**, 9660–9664.
22. Chou, C. L., Knepper, M. A., Hoek, A. N., Brown, D., Yang, B., Ma, T., and Verkman, A. S. (1999) *J. Clin. Invest.* **103**, 491–496.
23. Ma, T., Yang, B., Gillespie, A., Carlson, E. J., Epstein, C. J., and Verkman, A. S. (1998) *J. Biol. Chem.* **273**, 4296–4299.
24. Van Hoek, A. N., Ma, T., Yang, B., Verkman, A. S., and Brown, D. (2000) *Am. J. Physiol. Renal Physiol.* **278**, F310–F316.